Dihydrogen bonded phenol–borane-dimethylamine complex: An experimental and theoretical study

G. Naresh Patwari,[a] Takayuki Ebata, and Naohiko Mikami[b]
Department of Chemistry, Graduate School of Science, Tohoku University, Sendai 980-8578, Japan

(Received 26 November 2001; accepted 22 January 2002)

Continuing with our earlier communication on the dihydrogen bonded phenol–borane-dimethylamine complex [J. Chem. Phys. **113**, 9885 (2000)], we report here, the realistic structure of the said complex calculated using density functional theory at B3LYP/6-31 $++G(d,p)$ level. The agreement between the experimental and calculated vibrational spectrum for both the N–H and O–H stretching vibrations along with the low-frequency vibrations that appear in combination with O–H stretching, provides the basis for structural assignment. Analysis of the fate of B–H bonds and B–H stretching vibrations upon formation of dihydrogen bond reveals an anomalous behavior of average bond strengthening. © *2002 American Institute of Physics.* [DOI: 10.1063/1.1459415]

I. INTRODUCTION

Dihydrogen bonding essentially is an interaction, analogous to hydrogen bonding, between two oppositely charged hydrogen atoms and can be represented as $E–H(\delta-)\cdots(\delta+)H–X$, where E and X are electropositive and electronegative elements, respectively, with respect to hydrogen. More generally, the dihydrogen bond is formed when an acidic proton, X–H (X=N,O) interacts with a basic metal–hydrogen/boron–hydrogen σ-bond. The existence of dihydrogen bonding is known for little over a decade in the outer coordination sphere of some transition metal complexes,[1,2] wherein both inter- and intramolecular versions have been observed. Further, the dihydrogen bonding was also observed in the crystals of several borane-amines.[3] There are also several theoretical reports in the literature, which describe a variety of dihydrogen bonded complexes.[4–6] However, only recently we have identified the formation of dihydrogen bonded complexes in the gas phase,[7–9] including the phenol–borane-dimethylamine.[7]

It is well known that conventional hydrogen bonds are involved in molecular recognition and also as precursors to proton transfer reactions, which involve switching of σ bonds.[10] It is proposed that the dihydrogen bonding can be used in a similar fashion leading to selective stabilization of transition states, thereby increasing the reaction rates.[3] Further, crystal engineering of $[(GaH_2NH_2)_3]_2$ is an example of molecular recognition using dihydrogen bonds.[11] The dehydrogenation reactions, observed both in gas phase[12] and condensed phase,[13] are processes leading to σ-bond metathesis via the dihydrogen bonded intermediate. This motivates the present study, in which we look at the complex between phenol and borane-dimethylamine (BDMA), in a much wider perspective than reported earlier.

In this article we search for the realistic structure of phenol–BDMA through experimentally assisted density functional theory calculations. The comparison and agreement between the experimentally observed O–H and N–H stretching vibrations with the calculated values, forms the basis for the structural assignment. Further, we present two sets of secondary evidence based on (1) redshift in the electronic transition and (2) appearance of four large-amplitude low-frequency vibrations in combination with O–H stretching of phenol moiety. Finally, we examine the structural changes in the borane (BH_3) group of BDMA following dihydrogen bonding.

II. EXPERIMENTAL AND THEORETICAL METHODS

The details of complete experimental set up can be found elsewhere.[14] Briefly, the laser induced fluorescence (LIF) excitation, fluorescence detected infrared (FDIR) and IR–UV hole-burning spectra were recorded on jet-cooled mixture of phenol and BDMA. For this purpose, He at 4 bar was passed over phenol (Aldrich, vacuum sublimed) kept in a solvent holder at room temperature and was mixed with vapors of BDMA (Acros Organics) in a sample holder heated to 310 K and expanded using a pulsed nozzle of 0.8 mm diam. The LIF excitation spectrum of phenol was recorded without BDMA and then recorded again in the presence of BDMA. It follows, straightforwardly, that the new transitions appearing after the addition of BDMA are due to phenol–BDMA complexes. The FDIR spectroscopy is a technique, which can be used to record the IR spectrum of a particular species using its $S_1 \leftarrow S_0$ electronic transition as a selector. In this technique, an UV laser is fixed on electronic transition of the cluster of interest, which gives continuous fluorescence signal that reflects the ground-state population of the cluster in the jet. A tunable infrared pulse is introduced prior to the UV laser, which when resonant with the vibrational transition of the cluster, creates a population depletion in the ground state. The infrared absorption is then detected as a dip in the fluorescence signal, because of the population depletion. The IR–UV hole-burning spectroscopy was used to detect the presence of multiple isomers, if any, of the

[a]Electronic mail: naresh@qclhp.chem.tohoku.ac.jp
[b]Electronic mail: nmikami@qclhp.chem.tohoku.ac.jp

phenol–BDMA. This technique is an inverted version of FDIR spectroscopy. The hole-burnt spectra were recorded by fixing the frequency of IR laser to a vibrational transition of a specific cluster and tuning the UV laser. The fluorescence signal shows reduced intensity whenever the UV laser is resonant with the vibronic transitions of the selected cluster. Subtracting the hole-burnt spectrum from the LIF excitation spectrum allows to identify the transitions belonging to specific cluster. In our experiments the UV laser was a frequency doubled output of third harmonic Nd:YAG laser (Spectra Physics INDI-50) pumped dye laser (Lumonics HD-500) operating with Coumarin-540A dye. Tunable IR was produced by difference frequency generation (DFG) of second harmonic of the Nd:YAG laser (Quanta-Ray GCR/230) and the fundamental of second harmonic Nd:YAG (Quanta-Ray GCR/230) pumped dye laser (Continumm ND 6000; DCM dye) using a $LiNbO_3$ crystal. The typical laser powers for UV and IR were 100 and 500 μJ/pulse, respectively. The fluorescence was detected with a photomultiplier tube (Hamamatsu, 1P28) combined with a cutoff filter (Corning 7-54).

Density functional theory (DFT) based calculations were carried out with Becke's 3-parameter hybrid exchange correlation functional (B3LYP) (Ref. 15) using GAUSSIAN 98 (Ref. 16) to determine the structure of phenol–BDMA binary cluster. The basis set used for this purpose was a split valance $6\text{-}31++G(d,p)$ with diffuse and polarization functions on heavy atoms as well as hydrogens. It has been shown in several instances that inclusion of polarization and diffuse functions on heavy atoms improves the description of hydrogen bonding.[17] Since dihydrogen bonding is essentially hydrogen bonding between a pair of oppositely charged hydrogen atoms, polarization and diffuse functions were included on hydrogens as well. Moreover, usage of this level of theory is due to its acceptable accuracy for the dihydrogen bonded structures as exemplified in the case of BH_3-NH_3 and BH_3-H_2O dimers[4] and reasonable computational cost. The geometry optimizations for the monomers and the complexes were carried out under tight binding conditions without any constraints. The nature of the stationary point obtained on the potential energy surface (PES) was confirmed by calculating the vibrational frequencies at the same level of theory. The calculated vibrational frequencies were scaled by a factor of 0.955 to correct for the basis set truncation, partial neglect of the electron correlation and harmonic approximation and then compared with the experimentally observed values. The agreement between the calculated and observed vibrational frequencies served as a benchmark for the structural assignment. The stabilization energies were corrected for the zero point energy (ZPE) and the basis set superposition error (BSSE) using the counterpoise method.

III. RESULTS AND DISCUSSION

A. Spectra

The LIF excitation spectrum of phenol in the presence of BDMA is presented in Fig. 1. Upon addition of BDMA to the sample holder, we saw the emergence of several new transitions within 100 cm^{-1} to the red of phenol monomer band origin. Among the newly appeared transitions the most intense and lowest energy transition at 36269 cm^{-1}, marked "C," was assigned as band origin of the phenol–BDMA. We identified the mass number responsible for this transition as 153 amu, corresponding to the phenol–BDMA binary cluster, using time-of-flight mass spectrometry combined with the resonance enhanced multiphoton ionization technique. The band origin of phenol–BDMA is redshifted by 89 cm^{-1} from the corresponding band of bare phenol, which is rather small. This small redshift suggests the formation of π-electron bound complex. Several new transitions, which accompany the band origin, were assigned as vibronic bands of the same complex based on the IR–UV hole-burning spectroscopy, which will be presented later.

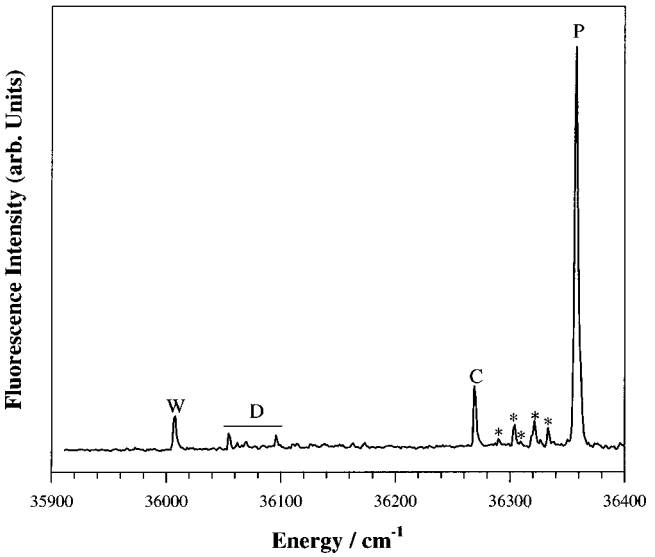

FIG. 1. LIF excitation spectrum of phenol in the presence of BDMA. The transition marked "C" is the band origin of phenol–BDMA complex and those marked with asterisk are the accompanying vibronic bands. The bands marked with "P," "W," and "D" are due to bare phenol, phenol–H_2O, and phenol dimer, respectively.

From the crystallographic data available for several borane-amines,[3] we expected phenol to be (di)hydrogen bonded to BDMA, because the B–H group is a strong and the only accessible proton acceptor site in BDMA. This would show a much larger redshift in the electronic transition, than that was observed. To confirm that nature of the phenol–BDMA complex, we recorded its IR spectrum using FDIR technique. The FDIR spectra of bare phenol and phenol–BDMA are displayed in Figs. 2(a) and 2(b), respectively. Bare phenol shows a single vibrational transition at 3657 cm^{-1} corresponding to O–H stretching and is in excellent agreement with that reported elsewhere.[14,18] The observed structure in the O–H vibrational transition is due to the fluctuation of IR power on account of ambient water vapor absorption. In the case of phenol–BDMA complex [Fig. 2(b)] the strongest transition at 3483 cm^{-1} was assigned to O–H stretching vibration of the complex, based on energy and intensity considerations. Four transitions on the higher frequency side of O–H stretching are combination bands with relative frequencies of 19, 31, 44, and 47 cm^{-1}, which are due to large-amplitude, low-frequency vibrations

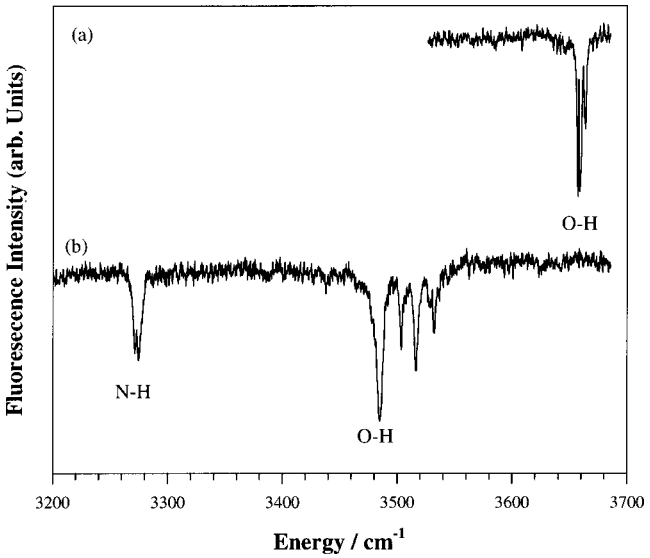

FIG. 2. FDIR spectra of (a) bare phenol and (b) phenol–BDMA complex.

involving intermolecular motions. The lowest energy vibrational transition, at 3272 cm^{-1}, is most likely to be the N–H stretching of the BDMA moiety. The splitting in this case is due to shot-to-shot instability of the IR laser. The O–H stretching vibration of phenol–BDMA is shifted by 174 cm^{-1} to a lower frequency a value much higher than in the case of phenol–H_2O (133 cm^{-1}) (Ref. 19) and clearly suggests that phenol is (di)hydrogen bonded to BDMA. We cannot compare the observed N–H stretching of the BDMA moiety to that in bare BDMA, since its gas phase IR spectrum is not known.

The existence of multiple isomers, even for the binary complexes, is known in many instances. To verify such an eventuality IR–UV hole-burning spectroscopy was carried out. Figure 3(a) shows the LIF excitation spectrum on an

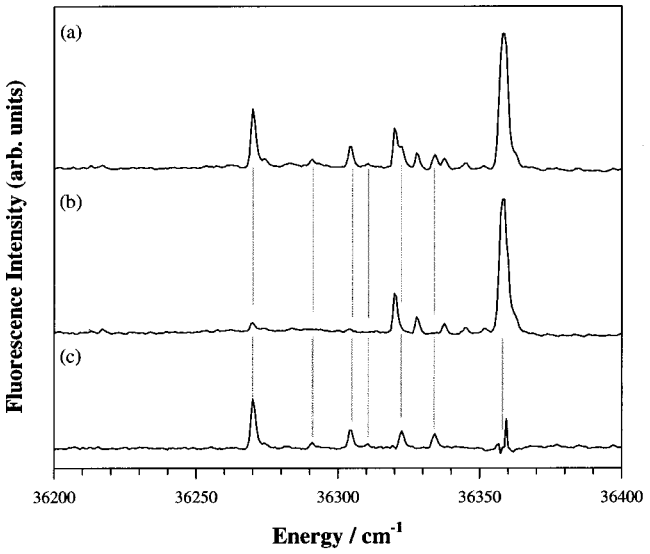

FIG. 3. (a) LIF excitation spectrum with IR off and (b) LIF excitation spectrum with the IR laser frequency fixed to the O–H stretching vibration of phenol–BDMA complex (IR–UV hole-burnt spectrum). (c) The difference spectrum obtained by subtracting (b) from (a).

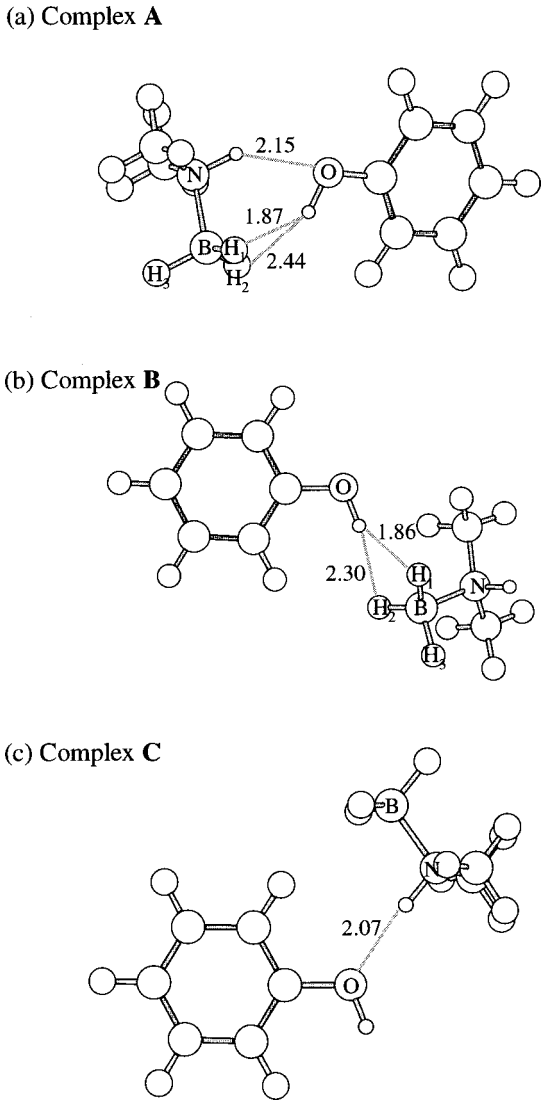

FIG. 4. Calculated structures of phenol–BDMA complexes obtained by using B3LYP/6-31++G(d,p) level of theory. Distances are in Angstroms and the labels B, N, O, and H correspond to boron, nitrogen, oxygen, and hydrogen atoms, respectively.

expanded scale, which is identical to that shown in Fig. 1. Figure 3(b) is the IR–UV hole-burnt spectrum, recorded by pumping the O–H stretching vibration of phenol–BDMA at 3483 cm^{-1}. It is clearly evident from this spectrum, apart from the band origin of the complex all the six newly appeared transitions are vanished or have diminished intensities. This confirms the presence of only one isomer of phenol–BDMA in the present experimental conditions. The difference spectrum shown in Fig. 3(c) [Fig. 3(a)–Fig. 3(b)] gives the LIF excitation spectrum of phenol–BDMA exclusively, which shows a rich vibronic activity in the low frequency region.

B. Calculated structures

The DFT-B3LYP/6-31++G(d,p) calculations gave three minima on the PES of phenol–BDMA, which are displayed in Figs. 4(a)–4(c) with their corresponding stabilization energies being −6.22, −4.37, and −3.58 kcal/mol, re-

spectively. The details of various contributions to the stabilization energy for all the three complexes are listed in Table I. The most stable complex [Fig. 4(a), complex **A**] forms a cyclic structure, with phenol acting both as a (di)hydrogen bond donor and a hydrogen bond acceptor. On the donor side, the phenolic proton is interacting with the B–H group of BDMA forming an O–H···H–B dihydrogen bond. For this dihydrogen bond the H···H contact distance is 1.87 Å while the B–H···H and O–H···H angles are 100.0° and 143.4°, respectively. In several borane-amines, whose crystal structures are reported in Cambridge Crystallographic Database (CSD), the dihydrogen bond has H···H contact distance of 1.7–2.2 Å, with a strongly bent B–H···H angle, averaging around 100° and near linear N–H···H with an average around 150°.[3] The geometrical parameters in the present case are very much in accordance with those reported in the CSD, and suggest the formation of dihydrogen bond. On the acceptor side, the acidic N–H of BDMA forms a conventional hydrogen bond with the phenolic oxygen lone pair. In this case the hydrogen bonded distance is 2.15 Å and the N–H···O angle is 139.2°. Because of the relatively long hydrogen bonded distance and the strongly bent angle, its contribution to the total stabilization energy will be minor.

The next stable complex is shown in Fig. 4(b) (complex **B**), in which the O–H group of phenol interacts with two B–H groups of BDMA forming a pair of bifurcated dihydrogen bonds of the type $O–H\cdots(H–B)_2$. In this structure the two H···H contact distances are 1.86, 2.30 Å, B–H···H angles are 100.0, 82.9° and the O–H···H angles are 150.1, 142.9°. Once again comparison with structures of borane-amines reported in CSD (Ref. 3) affirm the formation of dihydrogen bonds. The structure and stabilization energy of this complex is very much similar to the dihydrogen bonded phenol–borane-trimethylamine (phenol–BTMA).[8] Finally, the third minimum on the PES is a conventional hydrogen bonded complex, which is shown in Fig. 4(c) (complex **C**). In this complex, the acidic N–H of BDMA forms a hydrogen bond with the lone pair on phenolic oxygen with the hydrogen bonding distance of 2.07 Å and N–H···O angle being almost linear (176.5°). It may be noted that the structures of the complexes **A** and **C** are qualitatively very similar to those calculated at RHF/6-31G (*d, p*) level, reported in our earlier communication.[7] RHF calculations also converged on a structure similar to **B**, however, the vibrational frequency calculation gave an imaginary frequency, hence it was discarded.

C. Comparison between experiment and theory

Electronic and vibrational spectroscopic techniques do not give the geometrical parameters from which one can derive the structure directly. On the other hand, based on the spectral shifts in the electronic and vibrational transitions one can get hints about the structure and make an educated guess so as to what the structure can be. Phenolic O–H group acts both as an an acid and a base. In the electronic excited state the acidity of phenol increases while its basicity decreases which is the primary reason for the observed spectral shifts in the electronic transition upon complexation. On the other hand, the O–H stretching vibration of phenol moiety shows a considerable shift towards lower frequency whenever it is directly involved in hydrogen bonding. On the basis of these spectral characteristics, following can be realized for various phenol complexes. (1) In the case of van der Waals/π-electron bound complexes the electronic transition shows a small red shift, but the O–H stretching frequency remains almost unchanged, as in the case of phenol–Ar.[20] (2) If the phenol is a hydrogen bond donor, as in the case of phenol–H_2O, then the electronic transition show a substantial redshift, while the O–H stretching transition shows a substantial shift to a lower frequency.[19] (3) In the event of phenol acting as a hydrogen bond acceptor, as in the case of proton accepting site of phenol dimer, the electronic transition shows a blue shift[21] and the O–H stretching frequency remains almost unchanged.[22] The present phenol–BDMA complex shows a small redshift of 89 cm^{-1} in the electronic transition and a large shift of 174 cm^{-1} to a lower frequency in the O–H stretching vibration. Clearly, this does not fit to any of the cases described above. A survey of various hydrogen bonded clusters of phenol points towards the phenol–$(H_2O)_2$, which forms a cyclic structure with phenol acting as both a hydrogen bond donor and an acceptor. In this case the red shift in the electronic transition is only 133 cm^{-1} while the O–H stretching frequency shows a substantial shift of 269 cm^{-1} to a lower frequency.[19] This trend is very similar to that observed in the present case and extending the analogy it is reasonable to assume that phenol–BDMA forms a cyclic structure.

TABLE I. Stabilization energies (kcal/mol) along with various contributions for all the three isomers of phenol–BDMA calculated at the B3LYP/6-31++G(d,p) level.

Complex	ΔE_{el}	ZPE	BSSE	ΔE
A	−7.756	1.129	0.410	−6.217
B	−5.800	1.096	0.331	−4.373
C	−4.766	0.697	0.487	−3.582

From the stabilization energies of the complexes (see Table I), the upper limit for their relative abundance with nozzle temperature of 310 K is 1: 0.05: 0.01, if one does not account for the dynamic exchange between in the various isomers during the expansion. Therefore in all likelihood we would observe only the most stable complex, which clearly has at least 2 kcal/mol higher stabilization energy than the other two complexes, and indeed only one complex was observed. Further, the shift in the electronic transition for isomer **B** would be much larger to the red, and would be to the blue in the case of isomer **C**. From these two sets of information one can assign tentatively **A** as the probable structure of phenol–BDMA, as was done in our previous report.[7]

It has been long realized that the IR spectroscopy of stretching vibrations of protic groups, such as O–H, N–H, and sometimes even C–H, is the most important spectroscopic tool for the identification of hydrogen bonding.[23] This is due to the fact that these groups being involved directly are very sensitive to hydrogen bonded structures, and show a characteristic shift to a lower frequency upon hydrogen bonding. Comparison of the experimental with the calculated

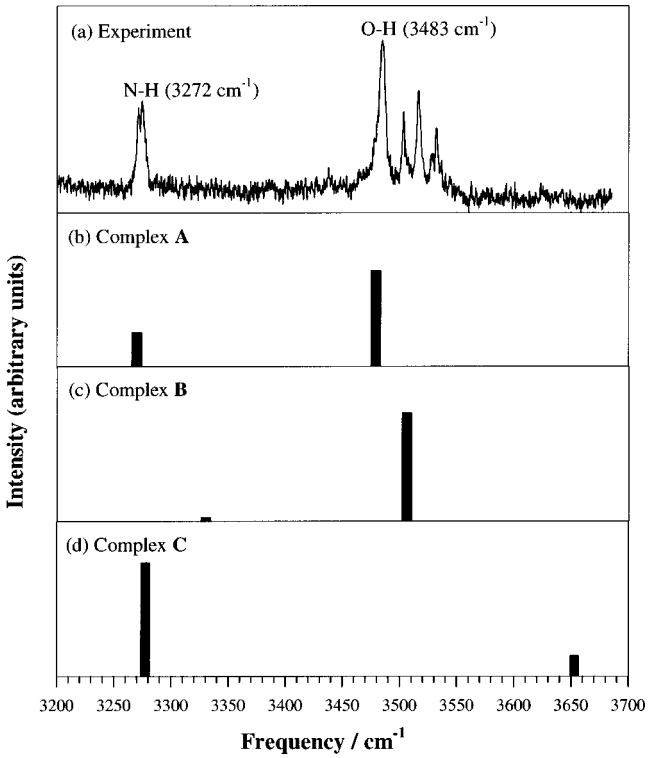

FIG. 5. Comparison of (a) FDIR spectrum of phenol–BDMA in the N–H and O–H stretching regions, with (b)–(d) calculated spectra corresponding to the complexes A–C, respectively.

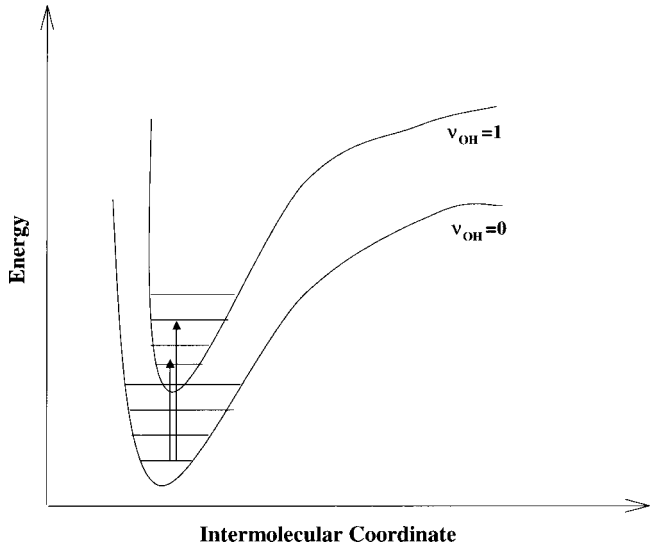

FIG. 6. Schematic potentials for the ground and excited vibrational states of ground electronic state along the intermolecular coordinate, illustrating the origin of combination bands. Due to change in shape and minimum in the potential with vibrational excitation combination bands are now Franck–Condon transitions between the two potentials.

vibrational spectrum provides the basis for the structural assignment, for the reason stated above. The comparison of experimental and calculated vibrational spectra is presented in Fig. 5. The top panel [Fig. 5(a)] shows the experimental spectrum, which is identical to one shown in Fig. 2(b), but is presented in an inverted ordinate, which reflects IR absorption. Next three panels, [Figs. 5(b)–5(d)] show the calculated vibrational (stick) spectra corresponding to the complexes **A**–**C**, respectively. Table II lists all the observed and calculated vibrational frequencies along with the calculated intensities. It is clearly evident from Fig. 5 and Table II that the agreement between the observed [Fig. 5(a)] and the calculated spectrum of complex **A** [Fig. 5(b)] is excellent, both in terms of frequencies and also the intensities. This clearly confirms that phenol–BDMA indeed has a cyclic structure in which phenol is both a (di)hydrogen bond donor and a hydrogen bond acceptor.

TABLE II. Calculated and experimental vibrational frequencies (cm^{-1}) in low-frequency and hydride stretching regions for all the three isomers of phenol–BDMA. Calculated intensities (km/mol) are given in parentheses. See text for details.

Description	A	B	C	Experiment[a]
Soft	17 (1.9)	22 (3.9)	13 (1.7)	19
Soft	35 (2.3)	31 (2.5)	29 (0.9)	31
Soft	42 (7.3)	41 (3.5)	42 (0.8)	44
Soft	50 (4.1)	51 (6.9)	57 (2.9)	47
N–H	3270 (156)	3330 (18)	3277 (294)	3272
O–H	3480 (437)	3506 (559)	3653 (53)	3483

[a]Experimental soft modes are defined with respect O–H stretching at 3483 cm^{-1}.

It is worth mentioning here that it has been found in several instances, the N–H stretching vibration of aliphatic amines has very small oscillator strength and is difficult to observe even with sensitive fluorescence detection (FDIR) or ion detection (RIDIR) techniques.[17,24] However, the N–H group in aliphatic amines gains substantial oscillator strength upon hydrogen bonding.[24] In the present phenol–BDMA complex, the N–H stretching vibration of the BDMA moiety has a substantial intensity, which suggests that it might be involved in hydrogen bonding. Among the three isomers of phenol–BDMA, the complexes **A** and **C** have hydrogen bonding between the N–H of BDMA and phenolic oxygen. This is reflected in higher calculated intensities in their respective spectra, in comparison with the isomer **B**. The observed intensity of N–H stretching vibration clearly indicates its involvement in the hydrogen bonding and supports the assignment of **A** as the structure of phenol–BDMA. Further, from the calculated vibrational frequencies, we note that the N–H stretching of BDMA moiety in phenol–BDMA shifts by 63 cm^{-1} to a lower frequency. However, unlike O–H stretching vibration, combination bands on N–H stretching are not observed. This is due to much weaker N–H$\cdots$O. hydrogen bonding interaction relative to the O–H$\cdots$H–B dihydrogen bond, which can be inferred from much lesser shifting to a lower frequency of the N–H stretching vibration (63 cm^{-1}) in comparison to the O–H stretching vibration (174 cm^{-1}).

The large-amplitude, low-frequency vibrational modes (soft modes) probed by stimulated Raman spectroscopy have been used for the structural identification of weakly bound complexes, because they sample the motions related to the intermolecular interaction.[25,26] The most notable examples are those of $(benzene)_n$ clusters[25] and also van der Waals and hydrogen bonded complexes of benzonitrile.[26] The final

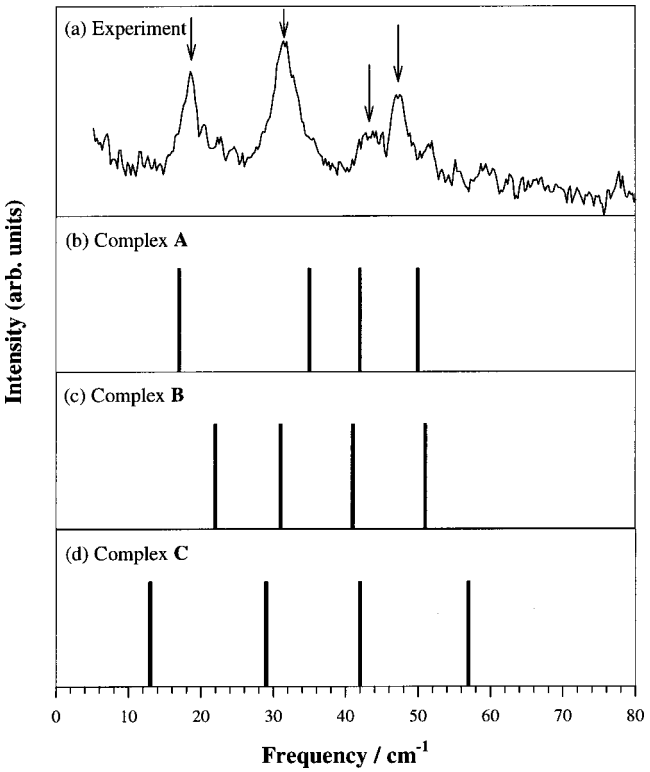

FIG. 7. Comparison of experimental and calculated IR spectra of the low frequency vibrations of phenol–BDMA. (a) Experimental spectrum, and (b)–(d) calculated spectra corresponding to the complexes A–C, respectively. The experimental spectrum is with respect to the O–H stretching vibration of the complex at 3483 cm^{-1} and the arrows indicate the peak positions. In the calculated spectra all the intensities are set to unity. See text for details.

piece of evidence comes from the soft modes, which were observed in the FDIR spectrum in combination with O–H stretching vibration. Though the vibrational selection rules do not allow combination bands, their occurrence has been reported in several hydrogen bonded complexes.[27,28] Figure 6 shows the schematic representation for the origin of combination bands. In the case of strong interaction between the hydrogen bond donor and acceptor, the shape and the minimum of the PES along the interaction/intermolecular coordinate changes with the O–H vibrational excitation, thereby creating a situation similar to that of electronic transitions. The combination bands therefore are Franck–Condon transitions between the ground and excited vibrational states of O–H stretching. The observed combination bands, therefore, are in principle soft modes of vibrationally excited state. Nevertheless, we compare the observed frequencies with those calculated for the ground vibrational state, with an assumption that the changes in the PES are not substantial upon vibrational excitation. This is indeed the case, because a large change in the PES would have given rise to progressions, which where not observed. Figure 7 shows the observed low-frequency vibrations [Fig. 7(a)] along with those calculated for all the three isomers [Figs. 7(b)–7(d)]. The frequencies are also listed in Table II along with the calculated intensities. In Fig. 7 all the calculated vibrations are presented with equal intensities. Since the transitions appear in combinations, it is not possible to calculate the intensities.

TABLE III. Comparison of various bond lengths (Å) of phenol, BDMA, and phenol–BDMA complexes. All the values are for the minima optimized at B3LYP/6-31++G(d,p) level of theory.

Bond	Phenol	BDMA	A	B	C
O–H	0.966		0.976	0.974	0.966
C–O	1.372		1.374	1.366	1.386
N–H		1.020	1.025	1.021	1.025
$B–H_1$		1.215	1.221	1.217	1.215
$B–H_2$		1.214	1.213	1.214	1.215
$B–H_3$		1.214	1.211	1.210	1.215
B–N		1.650	1.637	1.639	1.641

Therefore the comparison is only between the frequencies. At a first glance, it appears that all the three calculated spectra are in reasonable agreement with the observed spectrum. We examined $\Sigma(\Delta\nu)^2$, the summed square of the deviation between the observed and calculated values, which serves as a guideline to pick the right spectrum. The $\Sigma(\Delta\nu)^2$ values for the spectra 7(b), 7(c), and 7(d) are 33, 34, and 144, corresponding to the complexes **A**, **B**, and **C**, respectively. Even with some amount of uncertainty in accurately determining the peak positions in the experimental spectrum and due to the fact that the observed vibrations are the combination bands, on the basis of $\Sigma(\Delta\nu)^2$ values the possibility of third isomer being responsible for the observed low frequency vibrations can be absolutely ruled out. A closer look at the experimental spectrum spectra presented in Fig. 7(a), reveals that the first two vibrations are widely separated and the next two are much closer. Figure 7(b) also shows a very similar pattern. This implies that complex **A**, which is responsible for this spectrum is most likely to be the structure of phenol–BDMA.

D. Structural changes upon dihydrogen bonding

With the identification of the realistic structure of phenol–BDMA observed in supersonic jets, the next step is to look at the structural changes in phenol and BDMA upon complexation. This is very essential for the comprehensive understanding of dihydrogen bonding. Apart from the most stable structure, **A**, the observed phenol–BDMA complex, we also take a closer look at the next stable complex, **B**. This is due to fact that both the complexes are dihydrogen bonded. Furthermore, **B** has the structure very similar to phenol–BTMA,[8] which we have identified as a precursor for the dehydrogenation reaction from the dihydrogen bond, following resonant multiphoton ionization.[12]

Table III lists bond lengths of various groups for bare phenol and BDMA along with all the three phenol–BDMA complexes. The structure of **B** is discussed first, because in this complex phenol is just a (di)hydrogen bond donor and is much simpler. In the complex **B**, as a consequence of (di)hydrogen bonding the O–H bond of phenol is lengthened by 0.008 Å. On the other hand, the C–O bond is strengthened by 0.006 Å, which implies phenol acquires more quinoidal character upon (di)hydrogen bonding. These two changes are very similar to that observed in the case of phenol–H_2O.[29] This would directly translate to a decrease in O–H stretching and to an increase in C–O stretching frequencies. In the case

of BDMA moiety, the lengthening of the N–H bond is very small (less than 0.001 Å), which is expected, since the N–H is on the other side of interacting groups. Among the three B–H bonds, the one that is strongly dihydrogen bonded (1.86 Å H···H distance; B–H_1) is marginally elongated 0.002 Å, while the length of weakly dihydrogen bonded B–H bond (2.30 Å H···H contact distance; B–H_2) remains unchanged. However, contrary to our expectations, the noninteracting B–H bond (B–H_3) is shortened by 0.004 Å. Finally, the dative bonded B–N bond is considerably shortened, by 0.011 Å. This is because the electron density moves away from boron upon dihydrogen bonding, which is compensated by further electron donation from nitrogen (the amine lone pair, actually) thereby decreasing the bond distance. Similar changes were also seen in the case of phenol–BTMA.

In the case of the most form of stable phenol–BDMA, **A**, in which phenol is a (di)hydrogen bond donor and a hydrogen bond acceptor, the changes are more complicated. Both the O–H and C–O bonds of phenol moiety are lengthened by 0.01 and 0.002 Å, respectively, due to withdrawal of electron density both from the O–H bond and the oxygen lone pair, analogous to phenol–$(H_2O)_2$.[29] For the BDMA moiety the N–H bond lengthens by 0.004 Å, which, straightforwardly, is due to the hydrogen bond formation. Similar to the complex **B**, the length of B–H bond involved in dihydrogen bonding increases by 0.006 Å (B–H_1), while the other two noninteracting B–H bonds (B–H_2 and B–H_3) are shortened by 0.001 and 0.003 Å, respectively. In this case the B–H bond (B–H_3) farthest from the dihydrogen bonding site shortens the most. The B–N dative bond, once again shortens by 0.013 Å.

The structural changes of the interacting groups in the dihydrogen bond, both O–H and B–H, are very similar to those observed in the case of conventional hydrogen bonding. On the other hand, the non-interacting B–H bonds shorten. Further, we also note that in the case of the third, conventional hydrogen bonded complex, **C**, all the three B–H bond lengthen marginally, while the groups involved in hydrogen bonding show similar characteristics. It can also be seen from Table III that the maximum contraction of B–H bond happens in the complex **B**, which is purely (only) dihydrogen bonded. Further, the contraction of B–H bonds, which are not involved in dihydrogen bonding is very anomalous and should be further investigated.

E. The B–H stretching vibrations

The BH_3 group of BDMA has a C_3 local symmetry, which gives a lower frequency totally symmetric stretching (ν_1) and two higher frequency, near degenerate, nontotally symmetric stretching (ν_2 and ν_3) vibrations. The calculated values of ν_1, ν_2, and ν_3 for bare BDMA are 2329, 2371, and 2372 cm^{-1}, respectively. The formation of dihydrogen bonded complex lowers the local symmetry of the BH_3 group; consequently the vibrational levels get split. From the structural changes we have seen for the two dihydrogen bonded complexes **A** and **B**, we can expect the shifting of at least one of the B–H stretching vibration to a higher frequency.

Figure 8 shows the correlation diagram for the B–H stretching frequencies of BDMA upon complexation. The B–H stretching frequencies of BDMA and all the three phenol–BDMA complexes are also listed in Table IV. The situation of complex **C** is most straightforward. Since all the B–H bonds are marginally weakened, the complete manifold of B–H stretching vibrations is lowered with the center of the gravity shifting by -27 cm^{-1}. In the case of complex **B**, which is purely dihydrogen bonded complex, the stretching frequencies of interacting B–H bonds go down marginally (4, 6 cm^{-1}) while the frequency of the noninteracting B–H bond goes up by 22 cm^{-1}. This shifts the center of the gravity by $+12$ cm^{-1}, which implies that the average strength of the B–H bond actually increases with the formation of dihydrogen bonding. Since complex **A** can be regarded as an admixture of **B** and **C**, one would expect a frequency pattern similar to that of **B** but with center of the gravity lowered. This seems to be the case, however, lowering of the center of the gravity is -27 cm^{-1}, much higher than expected. The observed frequency pattern in **A** can also be explained as follows. The lowering of ν_1 is due to the dihydrogen bond formation. The remaining two B–H bonds are almost identical and has C_2 local symmetry thereby splitting into symmetric (ν_2) and antisymmetric stretching (ν_3). The actual situation could be a combination of both the effects giving rise to the observed pattern.

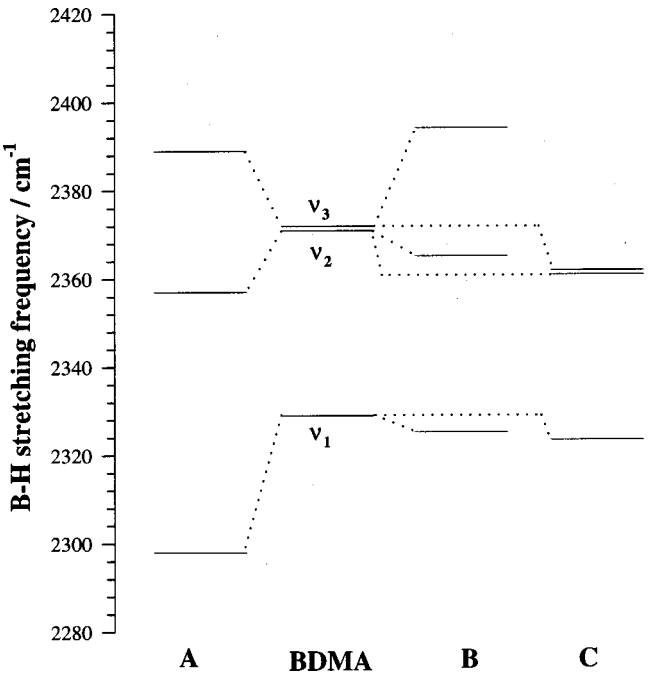

FIG. 8. Correlation diagram for the shifts in B–H stretching frequencies of BDMA upon complexation. See text for details.

TABLE IV. Calculated B–H stretching frequencies (cm^{-1}) of BDMA and phenol–BDMA complexes.

B–H stretch	BDMA	A	B	C
ν_1	2329	2298	2325	2323
ν_2	2371	2357	2365	2361
ν_3	2372	2389	2394	2361

IV. CONCLUDING REMARKS

All the four sets of data presented, namely, relative stabilization energies, spectral shifts in electronic and vibrational transitions, agreement between the experimental and calculated vibrational spectrum, and frequency matching between the observed and calculated soft modes, provides compelling evidence for the assignment of **A** as the realistic structure for the observed phenol–BDMA complex in the supersonic jet. Examination of the changes in individual molecules upon complexation reveals that the behavior of phenol is very much similar to that in other hydrogen bonded complexes. In the case of borane-amines, the B–H bond, which is involved in dihydrogen bonding, has similar characteristics to that of conventional hydrogen bonds, on the other hand, the noninteracting B–H bonds contract. In the case of purely dihydrogen bonded complex, **B**, the calculated vibrational frequencies suggest that the average strength of B–H bonds increases due to dihydrogen bonding.

In this article we have investigated the O–H stretching of the proton donating site together with the low frequency vibrations in the phenol–BDMA complex. However, comprehensive understanding of dihydrogen bonding will only be possible after the experimental observation of B–H stretching vibrations. Unfortunately, the current IR source in our laboratory does not cover the B–H stretching frequency region of 2300–2400 cm^{-1}. Efforts are being made in this direction and hopefully we will be able to investigate B–H stretching in the near future.

ACKNOWLEDGMENTS

G.N.P. thanks J.S.P.S. for the fellowship. T.E. acknowledges the support in part by the Grant-in-Aids for Scientific Research (No. 12640483) by J.S.P.S. N.M. acknowledges the support by Research for the Future, Photoscience (JSPS-RFTS-98P-01203). The authors also wish to thank Dr. A. Fujii, Dr. H. Ishikawa, and Dr. T. Maeyama for helpful suggestions and discussion.

[1] L. S. Van der Sluys, J. Eckert, O. Eisenstein, J. H. Hall, J. C. Huffman, S. A. Jackson, T. F. Koetzle, G. J. Kubas, P. J. Vergamini, and K. G. Caulton, J. Am. Chem. Soc. **112**, 4831 (1990).
[2] A. J. Lough, S. Park, R. Ramachandran, and R. H. Morris, J. Am. Chem. Soc. **116**, 8356 (1994).
[3] R. H. Crabtree, P. E. M. Siegbahn, O. Eisenstein, A. L. Rheingold, and T. Koetzle, J. Am. Chem. Soc. **29**, 348 (1996); W. T. Klooster, T. F. Koetzle, P. E. M. Siegbahn, T. B. Richardson, and R. H. Crabtree, J. Am. Chem. Soc. **121**, 6337 (1999).
[4] S. A. Kulkarni, J. Phys. Chem. A **102**, 7704 (1998); S. A. Kulkarni and A. K. Srivastava, *ibid.* **103**, 2836 (1999).
[5] S. J. Grabowski, Chem. Phys. Lett. **327**, 203 (2000).
[6] P. L. A. Popelier, J. Phys. Chem. A **102**, 1873 (1998).
[7] G. Naresh Patwari, T. Ebata, and N. Mikami, J. Chem. Phys. **113**, 9885 (2000).
[8] G. Naresh Patwari, T. Ebata, and N. Mikami, J. Chem. Phys. **114**, 8877 (2001).
[9] G. Naresh Patwari, T. Ebata, and N. Mikami, J. Phys. Chem. A **105**, 8462 (2001).
[10] G. A. Jeffery and W. Saenger, *Hydrogen Bonding in Biological Structures* (Springer, Berlin, 1994).
[11] J. P. Campbell, J. W. Hwang, V. G. Young, Jr., R. B. Von Dreele, C. J. Cramer, and W. L. Gladfelter, J. Am. Chem. Soc. **120**, 521 (1998).
[12] G. Naresh Patwari, T. Ebata, and N. Mikami, J. Phys. Chem. A **105**, 10753 (2001).
[13] J. L. Atwood, G. A. Koutsantonis, F. Lee, and C. L. Raston, J. Chem. Soc. Chem. Commun. **1994**, 91.
[14] S. Tanabe, T. Ebata, M. Fujii, and N. Mikami, Chem. Phys. Lett. **215**, 347 (1993).
[15] A. D. Becke, Phys. Rev. A **38**, 3098 (1988); C. Lee, W. Yang, and R. G. Parr, Phys. Rev. B **37**, 785 (1988).
[16] M. J. Frisch, G. W. Trucks, H. B. Schlegel *et al.*, GAUSSIAN 98, Revision A.7, Gaussian, Inc., Pittsburgh, PA, 1998.
[17] T. S. Zwier, J. Phys. Chem. A **105**, 8827 (2001).
[18] H. D. Bist, J. C. D. Brand, and D. R. Williams, J. Mol. Spectrosc. **24**, 413 (1967).
[19] T. Watanabe, T. Ebata, S. Tanabe, and N. Mikami, J. Chem. Phys. **105**, 408 (1996).
[20] A. Fujii, M. Miyazaki, T. Ebata, and N. Mikami, J. Chem. Phys. **110**, 11125 (1999).
[21] O. Dopfer, G. Lembach, T. G. Wright, and K. J. Muller-Dethlefs, J. Chem. Phys. **98**, 1933 (1993).
[22] T. Ebata, T. Watanabe, and N. Mikami, J. Phys. Chem. **99**, 5761 (1995).
[23] G. C. Pimentel and A. L. McClellan, *The Hydrogen Bond* (Freeman, San Francisco, 1960).
[24] G. Naresh Patwari (unpublished).
[25] M. W. Schaeffer, P. M. Maxton, and P. M. Felker, Chem. Phys. Lett. **224**, 544 (1994).
[26] R. Yamamoto, T. Ebata, and N. Mikami (unpublished).
[27] Y. Matsuda, T. Ebata, and N. Mikami, J. Chem. Phys. **110**, 8397 (1999).
[28] J. R. Carney, A. V. Fedorov, J. R. Cable, and T. S. Zwier, J. Phys. Chem. A **105**, 3487 (2001).
[29] H. Watanabe and S. Iwata, J. Chem. Phys. **105**, 420 (1996).